Detecting leaf chlorophyll content (LCC) using Sentinel-2 vegetation indices under different nitrogen conditions

Xuefeng Xu[1, *], Ali Mokhtari[1], Rachna Singh[1], Simon Vlad Luca[2], Mirjana Minceva[2], Kang Yu[1]

1. Precision Agriculture Lab, School of Life Sciences, Technical University of Munich, 85354 Freising, Germany

2. Biothermodynamics, School of Life Sciences, Technical University of Munich, 85354 Freising, Germany

A paper from the Proceedings of the
16th International Conference on Precision Agriculture
21-24 July 2024
Manhattan, Kansas, United States

Abstract.

Leaf chlorophyll content (LCC) is a significant indicator of photosynthetic performance and development status of plants. Remote sensing of crop chlorophyll often serves as a basic tool of crop nitrogen fertilization recommendation. The objective of the study is to explore how remote sensing can be utilized to more effectively monitor variations in crop growth, such as Leaf Chlorophyll Content (LCC). In this study, we investigated the performance of Sentinel-2 reflectance in (1) detecting the responses of wheat growth to different nitrogen conditions, and (2) estimating LCC to support nitrogen recommendation. LCC measurements were conducted over 2021 and 2022 at four sites under four nitrogen treatments (N1: 0 kg/ha, N2: 120 kg/ha, N3: 150 kg/ha, N4: 180 kg/ha). Thirty-eight vegetation indices (VIs) were selected and categorized into LAI-related and CHL-related index groups. They were calculated from Sentinel-2 spectral bands by Google Earth Engine (GEE). Univariate regression (UR) and Random Forest (RF) regression models were calibrated and validated, respectively on 70% and 30% of the entire dataset, for their capabilities in estimating LCC. Results showed that LCC was significantly different under four nitrogen treatments during the reproductive development stage (heading, flowering, and ripening), also across four sites. Under nitrogen deficiency, LCC was significantly lower than other nitrogen treatments. Based on UR models, VIs showed a large difference in explaining the variability in LCC with generally poor performance (R^2 = 0.01-0.37), but most of VIs performed well in explaining LAI (R^2 = 0.01-0.67). Both individual reflectance and VIS RF models successfully predicted LCC in the calibration and validation datasets (R2 greater than 0.95 and 0.59). The results indicate that LAI-related indices are indeed more sensitive to LAI, while CHL-related indices are more sensitive to CHL. However, few LAI-related VIs were also found to be related to LCC and showed significant differences between N treatments. NIR-related VIs are most strongly correlated with LCC, followed by red and red-edge bands. For predicting LCC, using B8 instead of B8A for NIR-related indices and B6 instead of B7 and B5 for red-edge-related indices may yield better results. Among soil background correction indices, SAVI exhibits stronger correlations with both LAI and CHL compared to OSAVI and GOSAVI. Finally, this research achieved the mapping of CHL distribution for 2021 and 2022, which can provide fertilizer

Xu, X. F., Mokhtari, A. & Yu, K. (2024). Detecting nitrogen deficiency and Leaf chlorophyll content (LCC) using Sentinel-2 vegetation indices. In Proceedings of the 16th International Conference on Precision Agriculture (unpaginated, online). Monticello, IL: International Society of Precision Agriculture.

recommendations to farmers to some extent.

Keywords.
chlorophyll spectral indices, precision nutrient management, nitrogen deficiency, precision farming, satellite remote sensing.

Introduction

Chlorophylls play a significant role in photosynthetic process, including light harvesting and energy conversion (Zarco-Tejada et al., 2002). Nitrogen (N) is the main ingredient of chlorophyll, and there is a close relationship between leaf chlorophyll content (LCC) and leaf nitrogen content (LNC). Crops generally absorb nitrogen from soil, as soil N supply is often limited, nitrogen fertilizer management should be adjusted to crop N requirements to optimize plant production (Nathalie et al., 2011; Muñoz-Huerta et al., 2013). Thus, accurate estimation of chlorophyll variations is important to help crop managers efficiently apply agrochemicals and fertilizers (Yu et al., 2014).

The traditional acquirement of leaf chlorophyll content data was usually conducted in the laboratory, which is destructive, time and labor-consuming (Hartmut & Alan, 1983). For portable and non-destructive measurement, few chlorophyll meters were developed, like SPAD-502 (Markwell et al., 1995; Zhang et al., 2022) and Dualex-4 (Cerovic et al., 2012). The essence of the chlorophyll meter is a measure of the greenness of leaves. To be representative, it required taking more readings in each region of interest (Dong et al., 2019). Moreover, the estimates of chlorophyll for the entire growing season are also less accurate. Remote sensing provides a practical approach to obtaining LCC across large scale. The red-edge bands, in particular, has a strong ability to predict chlorophyll (Clevers et al., 2001; Dash & Curran, 2004). Due to the high revisit frequency, Sentinel-2 can provide high temporal, spatial, and spectral resolution multi-spectral imageries. Especially it includes 3 red-edge bands (705 nm, 740 nm, and 783 nm) which are quite important for chlorophyll retrieval (Boochds et al., 1990; Drusch et al., 2012). Nevertheless, which red-edge band correlated more with chlorophyll is not clear yet.

Satellite vegetative indices (VIs) have been developed and well used to relate canopy reflectance with various crop parameters, like biomass, chlorophyll (CHL), and leaf area index (LAI) (Hatfield & Prueger, 2010; Hatfield et al., 2019). The calculation of VIs is simple and can be quickly used to estimate parameters in a wide range. Different indices exhibit varying performance under different conditions, as crop types, growth stages, nitrogen fertilizer treatments. The reflectance of plant canopy is a mixed pixel, which is comprehensively affected by the reflectance of underlying surfaces such as soil, and the structure of plant canopy (Huete et al., 2002; Hatfield et al., 2008). LAI is commonly used as one of the indicators to quantify vegetation canopy structure (Liang, 2004). The red-edge spectrum is influenced by both chlorophyll pigments and LAI, making it difficult to completely define and distinguish which indices are chlorophyll-related and which are LAI-related (Filella & Penuelas, 1994; Lamb et al., 2002). Chlorophyll related VIs are often dependent on the phenology, and they are also affected by various sources of variations other than chlorophyll (Cui et al., 2019). LAI related VIs are often highly connected to the above ground biomass, like NDVI (Anatoly et al., 2003). Therefore, understanding the capacity of chlorophyll-related indices and LAI-related indices to predict LCC and LAI, as well as the sensitivity of chlorophyll-related indices to LAI, is critical for selecting or developing indices that can improve the accuracy of chlorophyll predictions.

LCC can be used as an indicator to monitor differences in crop growth. The study's objectives were (1) to compare whether the current indices can be used to monitor wheat LCC levels under different conditions; (2) to evaluate how Sentinel-2 reflectance can monitor LCC more effectively; (3) to propose a strategy for estimating LCC of winter wheat using remotely sensed data; and (4) to map the LCC distribution to guide fertilization for farmers.

Materials and Methods

Field Measurements

The overall workflow of this study is shown in Figure 1. The field experiment was conducted at the Technical University of Munich, Germany (Freising, 50.7299°N, 7.0754°E). The soil is loam. The annual precipitation and average temperature are 505 mm and 7.6°C, respectively. The field samplings were conducted from 2021 to 2022 at four locations: Haunerfeld, Thalhausen, Schafhof and Grafenfeld. All of the fields were planted winter wheat and were applied 4 Nitrogen treatments in the spring, which were 0 kg N/ha (N1), 120 kg N/ha (N2), 150 kg N/ha (N3), and 180 kg N/ha (N4) in total.

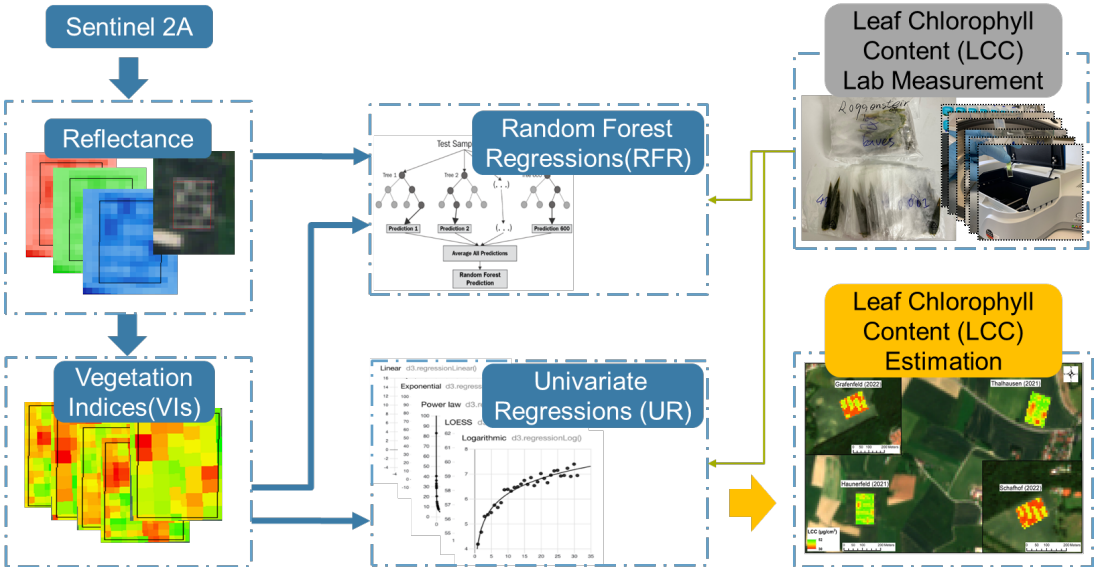

Fig 1. Overall workflow of this study.

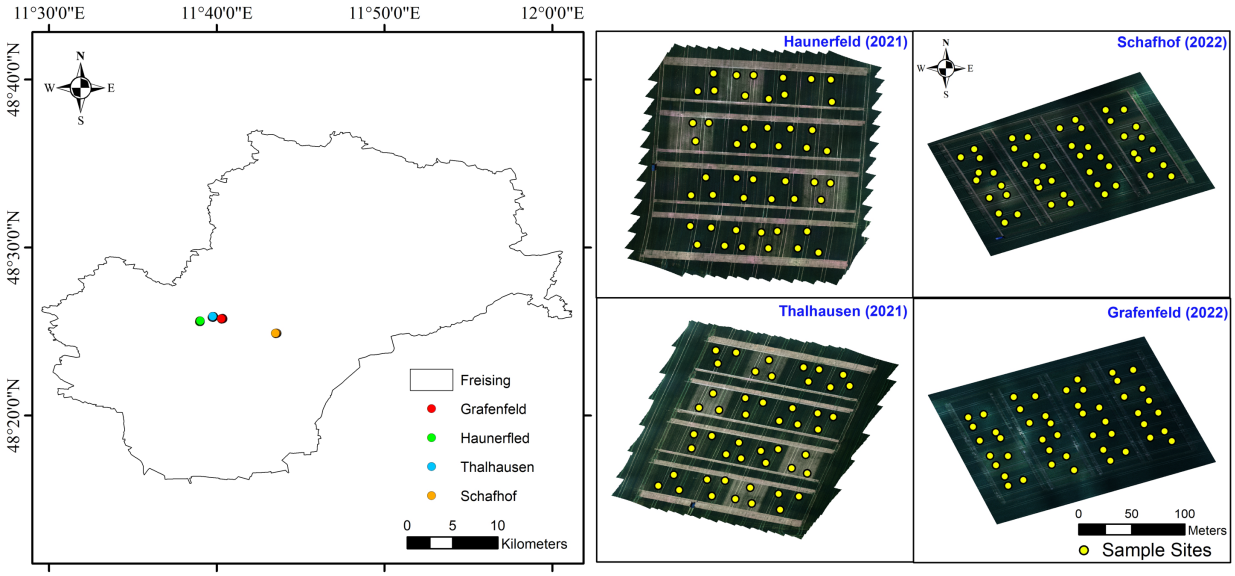

Fig 2. Locations of the study sites across southern Germany. The colorful dots in the left figure respectively show the four experimental sites in Freising, and the yellow dots in the right figures denote the field sampling sites.

Leaf samples and LAI data were taken from April to July in each year. The LAI data were collected by LAI-2000 Plant Canopy Analyzer. In this experiment, every field has 16 plots with a size of 900 m^2 (30 × 30 m). For every plot, 3 subsamples were evenly set and the GPS coordinates were recorded. During the entire growing season, sampling was conducted several times and the growth stages were recorded (Table 1). Three leaves and three times LAI were collected around

each spot for LCC measurement. The average of the three subsamples was taken as the final LCC of each plot.

Table 1. Fields, working years and dates, growth stage and number of sample points (n, 3 subsamples were averaged as 1 observation, i.e., sample point) of the study.

Year	Field	Sampling date	Growth Stage	n
2021	Haunerfeld	15.06.2021	Flowering	16
	Haunerfeld	22.06.2021	End of Flowering	16
	Haunerfeld	12.07.2021	End of Fruiting	16
	Thalhausen	14.06.2021	Flowering	16
	Thalhausen	28.06.2021	Beginning of Fruiting	16
	Thalhausen	21.07.2021	Ripening	16
2022	Schafhof	03.06.2022	End of Heading	16
	Grafenfeld	28.04.2022	Stem Elongation (SE)	16
	Grafenfeld	02.06.2022	End of Heading	16
	Grafenfeld	30.06.2022	Fruiting	16

Leaf Sampling and Chlorophyll Determination

The three leaf samples of each sampling site were collected and immediately frozen. The total chlorophyll content of each sample was extracted from 50 mg lyophilized material by 5 ml methanol, which was then filled up to 25 ml. After extraction, the absorbance of the extracts was measured with a UV-VIS spectrophotometer and the LCC was finally determined.

Remote Sensing Data

Sentinel-2A (S2A) images with 10 m spatial resolution obtained over the sites of interest in 2021 and 2022 were calculated to vegetation indices directly during the growing season from Google Earth Engine (GEE) (Google, 2002). The characteristics of the spectral bands (wavelength and bandwidth) are described on the GEE website. To avoid discrepancies between field measurements and radiometric information, the time difference between imaging and sampling was tried to minimize (Table 2).

Table 2. Comparison between sampling dates and S2A imaging dates

Year	Field	Sampling date	S2A imaging dates
2021	Haunerfeld	15.06.2021	15.06.2021
	Haunerfeld	22.06.2021	27.06.2021
	Haunerfeld	12.07.2021	12.07.2021
	Thalhausen	14.06.2021	15.06.2021
	Thalhausen	28.06.2021	27.06.2021
	Thalhausen	21.07.2021	20.07.2021
2022	Schafhof	03.06.2022	05.06.2022
	Grafenfeld	28.04.2022	03.05.2022
	Grafenfeld	02.06.2022	05.06.2022
	Grafenfeld	30.06.2022	30.06.2022

S2A Based Vegetation Indices (VIs)

Vegetation indices (VIs) have been related to various parameters and well used for vegetation monitoring. Among the parameters, chlorophyll content and LAI are highly connected to the estimation of leaf chlorophyll content. Thus, this research selected 38 vegetation indices and separated them into 2 groups: CHL-related and LAI-related indices (Table 3).

Table 3. Vegetation indices (VIs) used in the study. B2, B3, and B4 are blue, green, and red; B5, B6 and B7 are vegetation red-edge bands 1, 2 and 3, respectively. Both B8 and B8A are near infrared bands.

Group	Index	Name	Formula
CHL	MCARI1	Modified chlorophyll absorption reflectance index 1	((B5-B4)-0.2*(B5-B3))*(B5/B4) (Daughtry et al., 2002)
	MCARI2	Modified chlorophyll absorption reflectance index 2	((B6-B4)-0.2*(B6-B3))*(B6/B4) (Daughtry et al., 2002)
	MCARI3	Modified chlorophyll absorption reflectance index 3	((B7-B4)-0.2*(B7-B3))*(B7/B4) (Daughtry et al., 2002)
	CIre1	Red-edge 1 chlorophyll index	B8/B5-1 (Gitelson et al., 2005)
	CIre2	Red-edge 2 chlorophyll index	B8/B6-1 (Gitelson et al., 2005)
	CIre3	Red-edge 3 chlorophyll index	B8/B7-1 (Gitelson et al., 2005)
	CIgreen	Green chlorophyll index	B7/B3-1(Hatfield & Prueger, 2005)
	MND	Modified normalized difference	(B6-B2)/(B6+B5-2*B2) (Anatoly et al., 2003)
	Datt99	Datt99	(B8-B5)/(B8-B4) (Sims & Gamo, 2002)
	CSI	Chlorophyll sensitive index	2.5*[(B8-B5)/(B8+B5)]*(B2/B5) (Zhang et al., 2022)

	MTCI	MERIS terrestrial chlorophyll index	(B6-B5)/(B5-B4) (Dash & Curran, 2004)
	PSRI	Plant senescence reflectance index	(B4-B2)/B8 (Anatoly et al., 2003)
	IRECI	Inverted red-edge chlorophyll index	(B8-B4)/(B5/B6) (Frampton et al., 2022)
	Macc01	Maccioni 2001	(B7-B5)/(B7-B4) (Maccioni et al., 2022)
	NPCI	Normalized pigment chlorophyll ratio index	(B4-B2)/(B4+B2) (Hatfield & Prueger, 2005)
	TCI	Terrestrial chlorophyll index	(B6-B5)/(B5−B4) (Dash & Curran, 2004)
	TVI	Triangular vegetation index	0.5*(120*(B8-B3)-200*(B4-B3)) (Broge & leblanc, 2001)
	TCARI	Transformed chlorophyll absorption in reflectance index	3*((B5-B4)-0.2*(B5-B3)*(B5/B4)) (Haboudane et al., 2002)
	CVI	Chlorophyll vegetation index	(B8/B3)*(B4/B3) (Vincini, 2002)
	SR3	Simple ratio 3	B7/B6 (Gitelson et al., 1994)
	SR4	Simple ratio 4	B7/B5 (Gitelson et al., 1994)
	MCARI/OSAVI	MCARI/OSAVI	MCARI/OSAVI (Wu et al., 2008)
	TCARI/MSAVI	TCARI/MSAVI	TCARI/MSAVI (Haboudane et al., 2002)
	TCARI/OSAVI	TCARI/OSAVI	TCARI/OSAVI (Haboudane et al., 2002)
LAI	MCARI4	Modified chlorophyll absorption reflectance index 4	1.2*[2.5*(B8-B4)-1.3*(B8-B3)] (Haboudane et al., 2004)
	NDRE1	Red-edge 1 normalized difference vegetation index	(B6-B5)/(B6+B5) (Hatfield & Prueger, 2005)
	NDRE2	Red-edge 2 normalized difference vegetation index	(B7-B5)/(B7+B5) (Hatfield & Prueger, 2005)
	SR1	Simple ratio 1	B6/B4 (Gitelson et al., 1994)
	SR2	Simple ratio 2	B8/B4 (Gitelson et al., 1994)
	MSAVI	Modified soil adjusted vegetation index	$0.5*\{(2*B8+1)-\sqrt{(2*B8+1)^2-8*(B8-B4)}\}$ (Qi et al., 1994)
	DVI	Difference vegetation index	B8-B4 (Tucker, 1979)
	SAVI	Soil-adjusted vegetation index	(1+0.7)*(B8-B4)/(B8+B4+0.7) (Huete, 1988)
	OSAVI	Optimized soil adjusted vegetation index	(1+0.16)*(B8-B4)/(B8+B4+0.16) (Rondeaux, 1996)
	GOSAVI	Green optimized soil adjusted vegetation index	(1+0.16)*(B8-B3)/(B8+B3+0.16) (Rondeaux, 1996)
	GNDVI	Green normalized difference vegetation index	(B8-B3)/(B8+B3) (Gitelson, 1996)
	WDRVI	Wide dynamic range vegetation index	(0.3*B8-B4)/(0.3*B8+B4) (Gitelson, 2004)
	REIP	Red edge inflection point	705+35*((B4+B7)/2-B5)/(B6-B5) (Clevers, 2013)
	CCCI	Canopy chlorophyll content index	((B7-B5)/(B7+B5)]/[(B7-B4)/(B7+B4)) (Barnes et al., 2000)

Regression Models

Few regression models were tested to estimate LCC in this research: VI-based univariate models and Sentinel-2 based multivariate Random Forest (RF) models. The VIs were correlated with LCC by several UR models: linear, exponential, power, polynomial and logarithmic. Models were built using the 'lm' function in R environment. Table 4 showed the best performance and R^2 of different indices.

For RF models, one is using reflectance bands as input, and the other is using vegetation indices as input. Models were built in Python platform. We used a calibration and validation strategy to train the RF models. The dataset was randomly sampled for calibration (70%) and validation (30%). Since the size of the analysis dataset was limited (Table 1), the models were tested by splitting data 200 times for cross-validation []. The "RandomForestRegressor" package was used to build the models and a "n_estimators" was set to 200 which means the numbers of decision trees. The importance of predictor variables can be calculated to show which variables performed better.

The coefficient of determination (R^2) and root mean square error (RMSE) were using to assess the performances of the models, here are the equations:

$$R^2 = 1 - \frac{\sum_{i=1}^{n} (Obs_i - Mod_i)^2}{\sum_{i=1}^{n} (Obs_i - \overline{Obs})^2} \quad (1)$$

$$RMSE = \sqrt{\frac{\sum_{i=1}^{n} (Obs_i - Mod_i)^2}{n}} \quad (2)$$

where Obs_i and Mod_i are observed and modeled values, respectively, $\overline{Obs}$ and $\overline{Mod}$ are mean observed and modeled values, and n is the total number of samples.

Results and Discussion

Leaf Chlorophyll Content Distribution

In 2021, the average LCC for the entire growing season in Haunerfeld and Thalhausen was 41.89 and 20.51 μg/cm^2 respectively. In 2022, Grafenfeld had an average LCC of 38.91 μg/cm^2. Samples were collected only during the Heading stage in Schafhof in 2022, with an average LCC of 37.67 μg/cm^2. Due to substantial disparities in sampling times and locations across different sites and years, there are notable variations in LCC. LCC distribution varies significantly among different growing seasons and N treatments. However, with the exception of the stem elongation and ripening stages, LCC shows a significant increase with rising nitrogen application during the reproductive development stage (heading, flowering, and ripening). In early stem elongation stage, where nitrogen fertilizer has yet to affect the vegetation, the differences in LCC between N groups are not discernible. In the later ripening stage, LCC diminishes due to aging, thus making it challenging to assess. The LCC content of the N0 group, without any nitrogen application, notably lower from that of the other groups in reproductive stages, especially in flowering and fruiting.

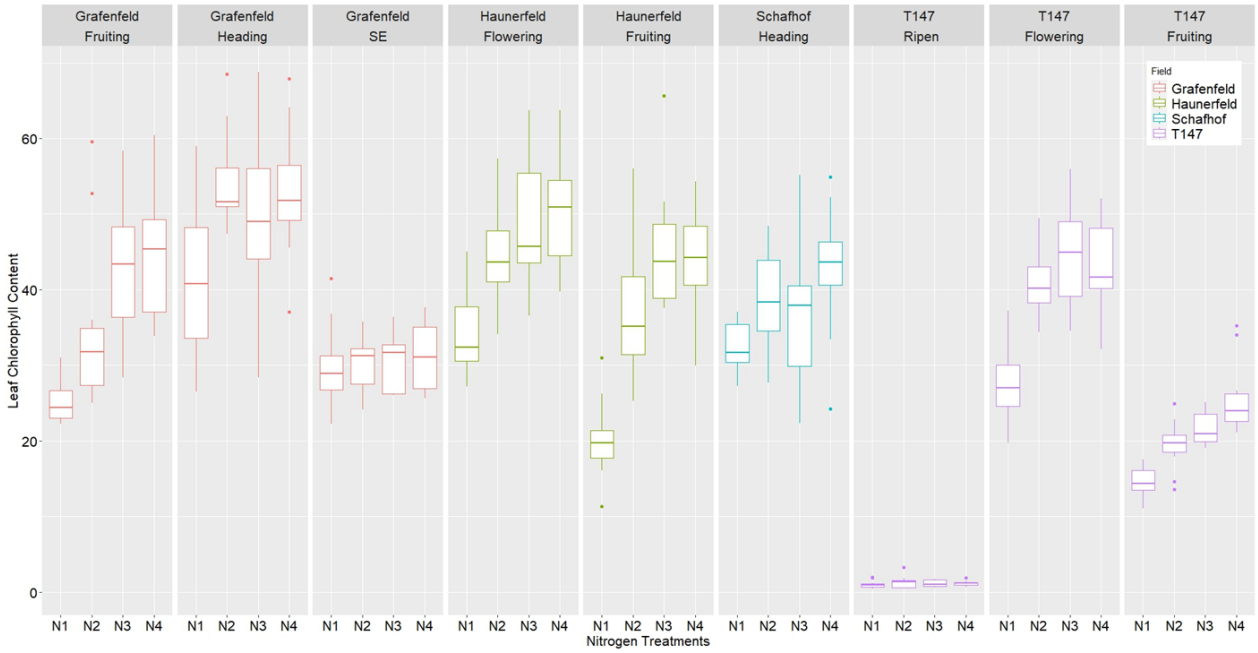

Fig 3. Leaf chlorophyll content distribution across different locations, Nitrogen treatments, and growing seasons.

Univariate regressions (UR)

The results of UR between LCC and VIS are shown in Table 4. Generally, the fits between VIs and LCC differed from moderate to poor depending on the VI. None of the R^2 values exceeded 0.375. Due to the models were using all samples, the results are not fits well. CIre2 and SR3 has the best performance with R^2 values in 0.375 and 0.353 using linear and polynomial functions, respectively. Among these VIs, NIR-related VIs had stronger correlations with LCC compared to others, also a little correlated with red and red-edge bands. SAVI has better performance than OSAVI and GOSAVI on LCC estimation. Among the top ten VIs, CHL-related indices work better than LAI-related indices.

Table 4. Results of univariate regressions between LCC and VIS. The sequence of VIs is sorted by the R^2 values with the order from largest to lowest values. The best performance model were also listed.

VIs	Model	R^2	RMSE	VIs	Model	R^2	RMSE
CIre2	linear	0.375	0.081	MCARI/OSAVI	exponential	0.181	0.435
SR3	polynomial	0.353	0.057	Datt99	polynomial	0.165	0.044
DVI	power	0.288	0.052	MND	polynomial	0.156	0.050
SAVI	power	0.287	0.063	CIre3	polynomial	0.152	0.049
MSAVI	power	0.284	0.074	GNDVI	exponential	0.133	0.102
TVI	power	0.274	3.412	WDRVI	linear	0.132	0.170

MCARI4	power	0.265	0.087	SR2	exponential	0.132	1.514
IRECI	power	0.262	0.153	TCARI/OSAVI	polynomial	0.131	0.061
CIre1	exponential	0.233	0.493	NDRE1	polynomial	0.128	0.065
MTCI	polynomial	0.215	1.213	MCARI2	power	0.123	0.209
OSAVI	exponential	0.213	0.086	CVI	linear	0.106	0.835
GOSAVI	exponential	0.210	0.077	CIgreen	polynomial	0.105	0.998
PSRI	logarithmic	0.209	0.044	TCARI	polynomial	0.104	0.025
MCARI3	exponential	0.205	0.374	Macc01	polynomial	0.091	0.049
SR4	polynomial	0.205	0.443	NPCI	logarithmic	0.085	0.087
NDRE2	polynomial	0.201	0.074	TCI	polynomial	0.077	0.780
TCARI/MSAVI	polynomial	0.196	0.065	SR1	exponential	0.073	1.021
REIP	polynomial	0.188	2.890	CCCI	polynomial	0.055	0.063
CSI	polynomial	0.186	0.158	MCARI1	polynomial	0.053	0.027

The relationship between LAI and VIs was also compared. The results of UR are shown in Table 5. In general, the fits between VIs and LAI differed from preferable to poor depending on the VI, which is better than the results of LCC. More than half of the fits between LAI and VIs are better than those with LCC. The R^2 results of the top ten VIs with LAI are all greater than 0.5. Among them, DVI, TVI, and MCARI4 performed the best, with all the R^2 greater than 0.65. Among the top ten indices which performed best with LAI, most of them were found that they are also the best-performing indices in the LCC UR model. Although CIre2 and SR3, which fit best with LCC, have lower R^2 values compared to other indices, they still show a strong correlation with LAI, with R^2 values of 0.467 and 0.401 respectively, even surpassing their performance with LCC.

Among the top 10 indices, LAI-related indices indeed have greater potential in predicting LAI, as evidenced by the fact that four out of the top five indices with the highest R^2 are LAI-related. However, it can be observed that CHL-related indices also have good potential in predicting LAI, such as TVI, PSRI, and CSI. Especially for CSI, although this index is proposed to be more sensitive to CHL while ignoring the influence of LAI (Zhang et al., 2022), our study found that it still has a strong correlation with LAI, with its R^2 with LAI even being higher than with CHL.

Table 5. Results of univariate regressions between LAI and VIS. The sequence of VIs is sorted by the R^2 values with the order from largest to lowest values. The best performance model were also listed.

VIs	Model	R^2	RMSE	VIs	Model	R^2	RMSE
DVI	Polynomial	0.668	0.044	NDRE 2	Power	0.409	0.087
TVI	Polynomial	0.656	3.022	SR 3	Polynomial	0.401	0.061
MCARI 4	Polynomial	0.649	0.078	WDRVI	Polynomial	0.387	0.157
SAVI	Polynomial	0.631	0.059	NDRE 1	Polynomial	0.374	0.072
MSAVI	Polynomial	0.610	0.069	SR 4	Power	0.371	0.471
PSRI	Polynomial	0.586	0.054	MCARI 1	Polynomial	0.360	0.024
IRECI	Polynomial	0.570	0.139	SR 2	Polynomial	0.307	1.383
CSI	Polynomial	0.537	0.145	SR 1	Polynomial	0.303	0.923
OSAVI	Polynomial	0.524	0.082	Datt99	Polynomial	0.291	0.064
MCARI 3	Power	0.506	0.379	GNDVI	Polynomial	0.287	0.093
MND	Linear	0.488	0.056	REIP	Polynomial	0.269	4.320
MCARI/OSAVI	Power	0.482	0.457	CIgreen	Polynomial	0.223	0.936
CIre 2	Polynomial	0.467	0.076	Macc01	Polynomial	0.222	0.072
NPCI	Polynomial	0.458	0.085	TCI	Polynomial	0.216	0.871
MCARI 2	Power	0.456	0.216	CCCI	Polynomial	0.201	0.080
CIre 1	Power	0.437	0.503	TCARI/MSAVI	Polynomial	0.124	0.074
TCARI	Power	0.431	0.027	CIre 3	Polynomial	0.102	0.051
GOSAVI	Polynomial	0.424	0.074	CVI	Polynomial	0.098	0.806
MTCI	Polynomial	0.411	1.217	TCARI/OSAVI	Polynomial	0.054	0.058

Random forest regressions

The results of RF models are shown in Table 5. This study used S2A reflectance directly and S2A calculated VIs as inputs, respectively. As mentioned before, 160 samples were collected in total. 70% including 112 samples were randomly selected for calibration and the left was used for validation. Both models showed good results, but reflectance model is a little better than VIs model. Overall, calibration accuracies were high, the R^2 and RMSE for the reflectance model are 0.957 and 3.131, respectively, while for the VIS model, they are 0.952 and 3.314, respectively. However, for the validation, the accuracies decreased. The R^2 for the reflectance and VIs model decreased to 0.701 and 0.589, and RMSE increased to 8.177 and 9.596.

Table 5. Results of random forest regressions.

	S2A reflectance		S2A VIs	
	Calibration (n=112)	Validation (n=48)	Calibration (n=112)	Validation(n=38)
R2	0.957	0.701	0.952	0.589

RMSE	3.131	8.177	3.314	9.596

Based on the importance analysis shown in Figure 4, the bands of near infrared (NIR) and red-edge and the related VIs (e.g., DVI, TVI, MND, CSI, CIre2) are the most important for the RF analysis. In the reflectance model, it can be found that the wavelength range of the near-infrared band B8 (832.8 nm) has better performance than that of B8A (864.7 nm). Among the three red edge bands, the spectral range of B7 (782.8 nm) and B6 (740.5 nm) is also better than that of B5 (704.1 nm) in estimating the leaf chlorophyll content (LCC). Therefore, in the VIS model, this study used the B8 band to calculate near-infrared related indices. In the VIS model, the B6 band seems to be the most suitable among the three red edge bands for applications in chlorophyll monitoring (e.g., NDRE2 performs better than NDRE1, and the same holds for MCARI2 and CIre2). Worth to notice, CIre2 and SR3 also play a significant role in the ranking of importance, which has similar results with linear model. Among the top 10 important indices, only DVI and MCARI4 belong to LAI related, which can illustrate the CHL-related indices are more related to LCC and showed significant differences between N treatments than LAI-related indices.

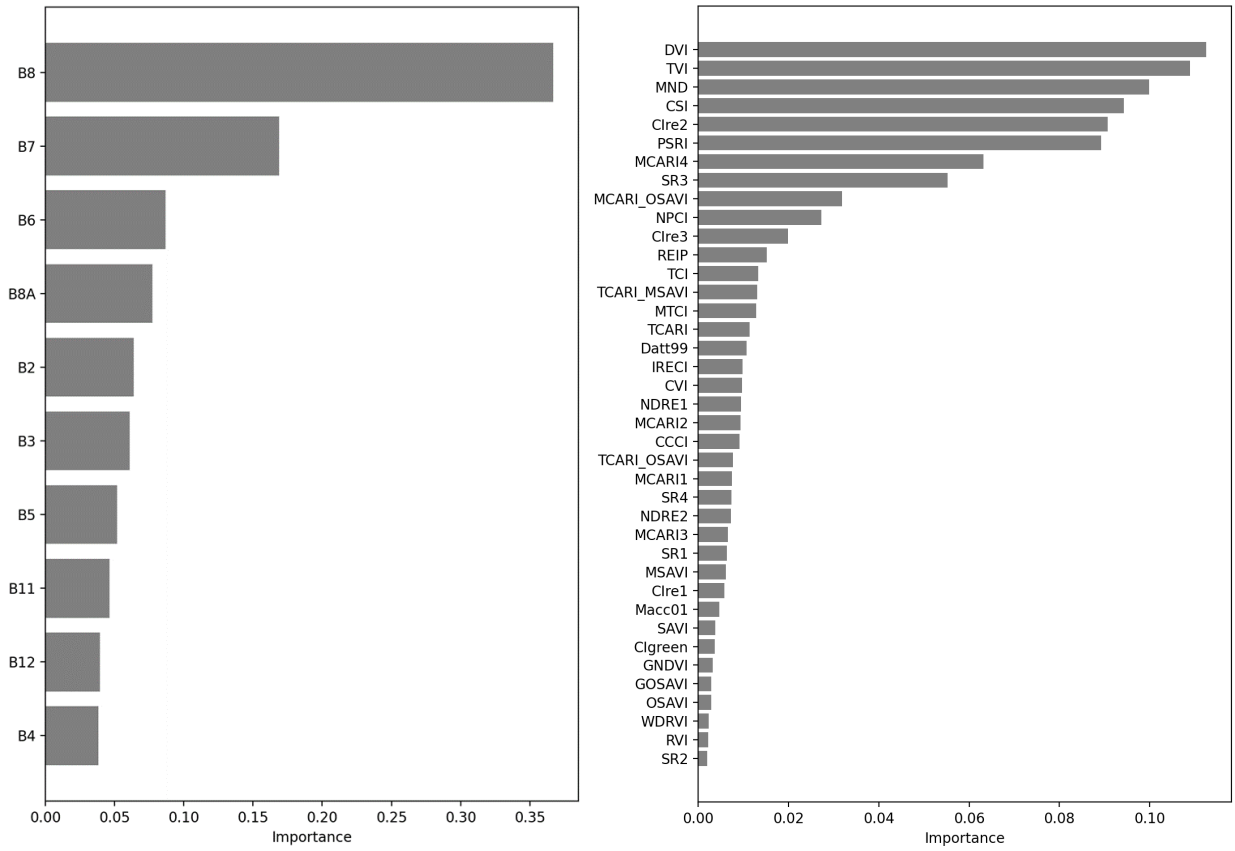

Fig 4. Importance of predictor variables (individual reflectance bands and vegetation indices) according to the random forest regression analysis in explaining the leaf chlorophyll content (LCC). The left figure showed the result of individual bands, and the right figure showed the VIs result.

Discussion

Comparison between models

Most VIs fitted preferable to moderately with LAI, especially the calibration R^2 of DVI and TVI are good, at 0.668 and 0.656 respectively. The proportion of VIs with calibration R^2 greater than 0.4 exceeds 50%. Vegetation indices fitted better with LAI than with LCC. Even though few VIs (e.g., CIre2 and SR3) fitted moderately with LCC (R^2 values for model calibration were 0.375 and 0.353), the overall VI-based UR performed inadequately (Table 4), which further indicates that the UR model was not suitable for LCC estimation. The differences of LCC among different nitrogen treatments were not significant at early and late stage, which may contribute to the poor

correlation. Moreover, due to the varied sampling dates across different growth stages and fields, and the influence of soil background on remote sensing images varies across different periods. This makes it challenging to build robust models based on simple VIs to accommodate such uneven conditions.

Compared to UR, RF models show significantly better performance in LCC estimation. Its most notable enhancement over UR is its ability to manage multiple variables within a single model, leveraging more information and intuitive output the variable importance. In this study, RF models achieved higher overall accuracy, with slightly better calibration and validation for single band reflectance model than VIs model (Table 5). RF exhibits clear advantages such as simplicity of operation, high efficiency, and robust reliability.

Comparison between VIs

All models indicate that CHL-related indices are better at monitoring LCC variations under different conditions compared to LAI-related indices. The results of the UR model indeed show that LAI-related indices are more sensitive to LAI, while CHL-related indices are more sensitive to LCC. However, CHL-related and LAI-related indices cannot be completely separated. As CIre2 and SR3 are CHL-related indices, but they exhibit higher correlation in predicting LAI than in predicting LCC.

Among soil background correction indices, SAVI exhibits stronger correlations with LAI compared to OSAVI and GOSAVI. But at the meantime, soil correction indices also show strong potential in predicting LAI. For instance, SAVI, MSAVI, and OSAVI all rank in the top ten in terms of R^2 in the UR model with LAI.

NIR-related VIS indices are strongly correlated with LCC, followed by the red and red-edge bands. When applying indices to predict LCC, calculations using B8 instead of B8A for NIR-related indices and B6 instead of B7 and B5 for red-edge-related indices may yield better results. Considering all models, indices such as CIre2, SR3, DVI, TVI, MND, and CSI appear to have better predictive capabilities for LCC.

Spatial distribution of Leaf chlorophyll content

Due to the higher accuracy of the RF reflectance model, and significant differences in LCC were observed among different nitrogen treatments during the flowering and fruiting growth stages. Instantaneous LCC during these two growth periods within the study area can be plotted (Figure 5). Using Google Earth Engine (GEE), images for June 17th, 2021, and June 27th, 2022, were downloaded to predict the spatial distribution of LCC during the fruiting period in 2021 for Haunerfeld and Thalhausen, and during the flowering period in 2022 for Grafenfeld and Schafhof. From the map, farmers can potentially identify variations in LCC within and between fields. By comparing different nitrogen treatments, it was found that wheat LCC under the 0 kg N/ha condition was significantly lower than other groups, while LCC under the 180 kg N/ha condition was not markedly higher than other groups. Over-fertilization not only wastes resources but also burdens the land with environmental pollution. Comparing LCC under the 120 and 150 kg N/ha treatments, they were generally at similar levels, with LCC slightly higher under the 150 kg N/ha condition compared to 120 kg N/ha, but the difference was not distinct. From the perspective of environmentally sustainable resource utilization, the 120 kg N/ha treatment appears to be the most cost-effective option.

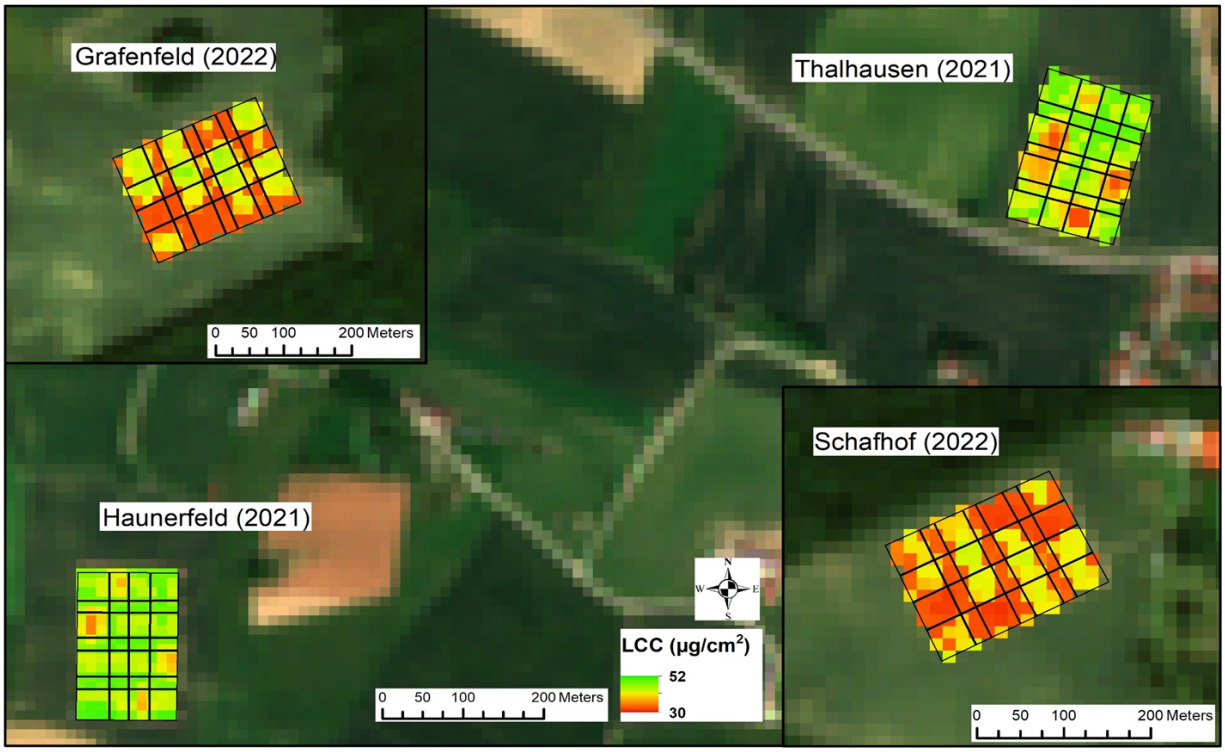

Fig 5. Layout of the estimated leaf chlorophyll content (LCC) from Sentinel-2 imagery obtained on 17 June 2021 (for Haunerfeld and Thalhausen, in flowering stage) and 27 June 2022 (for Grafenfeld and Schafhof, in fruiting stage), using the RF reflectance model. The background imagery are Sentinel-2 imageries of the two dates above mentioned.

This study enables precise prediction of LCC. By monitoring changes and distribution of LCC levels, it aids farmers in assessing plant growth and nutrient status, thereby providing valuable fertilizer recommendations.

Conclusions

(i) LCC estimation of flowering and fruiting stages in southern Germany from Sentinel-2 data using univariate and multivariate regression models was tested in this study. The results demonstrate precise in-season LCC estimation by the random forest algorithm. Random forest models performed better than the univariate models in terms of accuracy. Using individual reflectance of RF regression is a little better compared to utilizing vegetation indices.

(ii) It was challenging to develop a sufficiently robust univariate model to estimate crop LCC by directly using Sentinel-2 based vegetation indices. Due to the varied sampling dates across different growth stages and fields, achieving more accurate estimation of LCC throughout the phenological cycle remains challenging with the current vegetation indices. Given the time and labor consuming of sampling, the existing dataset is relatively limited. Establishing a larger dataset could address this issue, thus necessitating continuous resources and possible international collaboration for further data collection. Verified results indicate that CHL-related indices are more effective in monitoring dynamic changes in LCC compared to LAI-related indices. However, how to use these indices more accurately and efficiently to monitor LCC will be the next focus of our study.

(iii) The estimated distribution of LCC fitted well with the Nitrogen fertilization treatments. The methods established in this study could be used to assist farmers in monitoring crop health status and making decisions on fertilization.

References

Anatoly, A. G., Andrés, V., Timothy J. ., Donald, C. R., Galina, K., & Bryan, L. (2003). Remote

estimation of leaf area index and green leaf biomass in maize canopies. *Geophysical Research Letters*, 30(5), 1248. https://doi.org/10.1029/2002GL016450

Anatoly, A. G., Yuri, G., & Mark, N. M. (2003). Relationships between leaf chlorophyll content and spectral reflectance and algorithms for non-destructive chlorophyll assessment in higher plant leaves. *Journal of Plant Physiology*, 160(3), 271-282. https://doi.org/10.1078/0176-1617-00887

Barnes, E. M., Clarke, T., Richards, S. E., Colaizzi, P. D., Haberland, J., Kostrzewski, M., Waller, P. M., Choi, C. Y., Riley, E., Thompson, T. L., Lascano, R. J., Li, H., Moran, M. S., Robert, P. C., Rust, R. H., & Larson, W. E. (2000). Coincident detection of crop water stress, nitrogen status and canopy density using ground-based multispectral data. *In Proceedings of the Fifth International Conference on Precision Agriculture*, Bloomington, IN, USA, 16–19 July 2000; 6–20.

Boochds, F., Kupfer, G., Dockter, K., & Kuehbauch, W. (1990). Shape of the red edge as vitality indicator for plants. *International Journal of Remote Sensing*, *11*(10), 1741–1753. https://doi.org/10.1080/01431169008955127

Broge, N. H., Leblanc, E. (2001). Comparing prediction power and stability of broadband and hyperspectral vegetation indices for estimation of green leaf area index and canopy chlorophyll density. *Remote Sensing of Environment*, 76(2), 156-172. https://doi.org/10.1016/S0034-4257(00)00197-8

Cerovic, Z. G., Masdoumie, G., Ghozlen, N. B., & Latouche, G. (2012). A new optical leaf-clip meter for simultaneous non-destructive assessment of leaf chlorophyll and epidermal flavonoids. *Physiologia Plantarum*, 146(3), 251-60. doi: 10.1111/j.1399-3054.2012.01639.x

Clevers, J.G.P.W., de Jong, S.M., Epema, G.F., van der Meer, F., Bakker, W.H., Skidmore, A.K., & Addink, E.A. (2001). MERIS and the red-edge position. *International Journal of Applied Earth Observation and Geoinformation*, 3(4), 313-320. https://doi.org/10.1016/S0303-2434(01)85038-8

Clevers, J. G. P. W. & Gitelson, A.A. (2013). Remote estimation of crop and grass chlorophyll and nitrogen content using red-edge bands on Sentinel-2 and -3. *International Journal of Applied Earth Observation and Geoinformation*. 23, 344-351. https://doi.org/10.1016/j.jag.2012.10.008

Cui, B.; Zhao, Q.; Huang, W.; Song, X.; Ye, H.; & Zhou, X. (2019) A New Integrated Vegetation Index for the Estimation of Winter Wheat Leaf Chlorophyll Content. *Remote Sens*, 11, 974. https://doi.org/10.3390/rs11080974

Dash, J., & Curran, P. J. (2004). The MERIS terrestrial chlorophyll index. *International Journal of Remote Sensing*, 25(23), 5403–5413. https://doi.org/10.1080/0143116042000274015

Daughtry, C. S. T, Walthall, C. L., Kim, M.S, Brown de Colstoun, E., McMurtrey III, J.E. (2000). Estimating corn leaf chlorophyll concentration from leaf and canopy reflectance. *Remote Sensing of Environment*, 74(2), 229-239. https://doi.org/10.1016/S0034-4257(00)00113-9

Dong, T., Shang, J., Chen, J.M., Liu, J., Qian, B., Ma, B., Morrison, M.J., Zhang, C., Liu, Y., Shi, Y., & et al. (2019). Assessment of Portable Chlorophyll Meters for Measuring Crop Leaf Chlorophyll Concentration. *Remote Sensing*, 11, 2706. https://doi.org/10.3390/rs11222706

Drusch, M., Bello, U. D., Carlier, I. S., Colin, O., Fernandez, V., Gascon, F., Hoersch, B., Isola, C., Laberinti, P., & Martimort, P. (2012). Sentinel-2: esa's optical high-resolution mission for GMES operational services. *Remote Sensing of Environment*, 120, 25-36. https://doi.org/10.1016/j.rse.2011.11.026

Filella, I., & Penuelas, J. (1994). The red edge position and shape as indicators of plant chlorophyll content, biomass and hydric status. *International Journal of Remote Sensing*, 15(7), 1459–1470. https://doi.org/10.1080/01431169408954177

Frampton, W. J., Dash, J., Watmough, G., & Milton, E. J. (2013). Evaluating the capabilities of Sentinel-2 for quantitative estimation of biophysical variables in vegetation. *ISPRS Journal of Photogrammetry and Remote Sensing*, 82, 83-92. https://doi.org/10.1016/j.isprsjprs.2013.04.007

Gitelson, A. A., & Merzlyak, M. N. (1994). Spectral reflectance changes associated with autumn senescence of Aesculus hippocastanum L. and Acer platanoides L. leaves - spectral features and relation to chlorophyll estimation. *Journal of Plant Physiology*, 143(3), 286-292. https://doi.org/10.1016/S0176-1617(11)81633-0

Gitelson, A. A., Kaufman, Y.J., & Merzlyak, M. N. (1996). Use of a green channel in remote sensing of global vegetation from EOS-MODIS. *Remote Sensing of Environment*, 58(3), 289-298. https://doi.org/10.1016/S0034-4257(96)00072-7

Gitelson, A. A. (2004). Wide dynamic range vegetation index for remote quantification of biophysical characteristics of vegetation. *Journal of Plant Physiology*, 161(2), 165-173. https://doi.org/10.1078/0176-1617-01176

Gitelson, A. A., Viña, A., Ciganda, V., Rundquist, D. C., & Arkebauer, T. J. (2005). Remote estimation of canopy chlorophyll content in crops. *Geophysical Research Letters*, 32, L08403. doi:10.1029/2005GL022688.

Google. (2024). *Google Earth Engine. Net.* https://earthengine.google.com/

Haboudane, D., Miller, J. R., Tremblay, N., Zarco-Tejada, P. J., & Dextraze, L. (2002). Integrated narrow-band vegetation indices for prediction of crop chlorophyll content for application to precision agriculture. *Remote Sensing of Enviroment*, 81(2-3), 416-426. https://doi.org/10.1016/S0034-4257(02)00018-4

Haboudane, D., Miller, J. R., Pattey, E., Zarco-Tejada, P. Z., & Strachan, I. B. (2004). Hyperspectral vegetation indices and novel algorithms for predicting green LAI of crop canopies: Modeling and validation in the context of precision agriculture. *Remote Sensing of Environment*, 90(3), 337-352. https://doi.org/10.1016/j.rse.2003.12.013

Hartmut, K. L., & Alan. R. W. (1983). Determinations of total carotenoids and chlorophylls a and b of leaf extracts in different solvents. *Biochemical Society Transactions*, 11(5), 591–592. https://doi.org/10.1042/bst0110591

Hatfield, J. L., Gitelson, A. A., Schepers, J. S., & Walthall, C. L. (2008). Application of Spectral Remote Sensing for Agronomic Decisions. *Agronomy Journal*, 100(53), 117-131. https://doi.org/10.2134/agronj2006.0370c

Hatfield, J.L., & Prueger, J.H. (2010). Value of Using Different Vegetative Indices to Quantify Agricultural Crop Characteristics at Different Growth Stages under Varying Management Practices. *Remote Sensing*, 2(2), 562-578. https://doi.org/10.3390/rs2020562

Hatfield, J.L., Prueger, J.H., Sauer, T.J., Dold, C., O'Brien, P., & Wacha, K. (2019). Applications of Vegetative Indices from Remote Sensing to Agriculture: Past and Future. *Inventions*, 4, 71. https://doi.org/10.3390/inventions4040071

Huete, A.R. (1988). A soil vegetation adjusted index (SAVI). *Remote Sensing of Environment*, 25(3), 295-309. https://doi.org/10.1016/0034-4257(88)90106-X

Huete, A., Didan, K., Miura, T., Rodriguez, E.P, Gao, X., & Ferreira, L.G. (2002). Overview of the radiometric and biophysical performance of the MODIS vegetation indices. *Remote Sensing of Environment*, 83(1–2), 195-213. https://doi.org/10.1016/S0034-4257(02)00096-2

Lamb, D. W., Steyn-Ross, M., Schaare, P., Hanna, M. M., Silvester, W., & Steyn-Ross, A. (2002). Estimating leaf nitrogen concentration in ryegrass (Lolium spp.) pasture using the chlorophyll red-edge: Theoretical modelling and experimental observations. *International Journal of Remote Sensing*, 23(18), 3619–3648. https://doi.org/10.1080/01431160110114529

Liang, S. (2004). *Quantitative remote sensing of land surfaces*. Wiley, Hoboken.

Maccioni, A., Agati, G., & Mazzinghi, P. (2001). New vegetation indices for remote measurement of chlorophylls based on leaf directional reflectance spectra. *Journal of Photochemistry and Photobiology B: Biology*, 61(1-2), 52-61. https://doi.org/10.1016/S1011-1344(01)00145-2

Markwell, J., Osterman, J.C. & Mitchell, J.L. (1995). Calibration of the Minolta SPAD-502 leaf chlorophyll meter. *Photosynthesis Research,* 46, 467–472. https://doi.org/10.1007/BF00032301

Muñoz-Huerta, R.F., Guevara-Gonzalez, R.G., Contreras-Medina, L.M., Torres-Pacheco, I., Prado-Olivarez, J., & Ocampo-Velazquez, R.V. (2013). A Review of Methods for Sensing the Nitrogen Status in Plants: Advantages, Disadvantages and Recent Advances. *Sensors*, 13, 10823-10843. https://doi.org/10.3390/s130810823

Nathalie, V., Martin, E., Gilles, R., & Pierre, R. (2011). Potential of field hyperspectral imaging as a non destructive method to assess leaf nitrogen content in Wheat. *Field Crops Research*, 122(1), 25-31. https://doi.org/10.1016/j.fcr.2011.02.003

Qi, J., Chehbouni, A., Huete, A.R., Kerr, Y.H., & Sorooshian, S. (1994). A modified soil adjusted vegetation index. *Remote Sensing of Environment*, 48(2), 119-126. https://doi.org/10.1016/0034-4257(94)90134-1

Rondeaux, G. (1996). Optimization of soil-adjusted vegetation indices. *Remote Sensing of Environment*, 55(2), 95-107. https://doi.org/10.1016/0034-4257(95)00186-7

Sims, D. A., & Gamon, J. A. (2002). Relationships between leaf pigment content and spectral reflectance across a wide range of species, leaf structures and developmental stages. *Remote Sensing of Environment*, 81(2-3), 337-354. https://doi.org/10.1016/S0034-4257(02)00010-X

Tucker, C.J. (1979). Red and photographic infrared linear combinations for monitoring vegetation. *Remote Sensing of Environment,* 8(2), 127-150. https://doi.org/10.1016/0034-4257(79)90013-0

Vincini, M. (2008). A broad-band leaf chlorophyll vegetation index at the canopy scale. *Precision Agriculture*, 9, 303-319. https://doi.org/10.1007/s11119-008-9075-z

Wu, C. Y., Niu, Z., Tang, Q., & Huang, W. J. (2008). Estimating chlorophyll content from hyperspectral vegetation indices: Modeling and validation. *Agricultural and Forest Meteorology*, 148(8-9), 1230-1241. https://doi.org/10.1016/j.agrformet.2008.03.005

Yu, K., Leufen, G., Hunsche, M., Noga, G., Chen, X., & Bareth, G. (2014). Investigation of Leaf Diseases and Estimation of Chlorophyll Concentration in Seven Barley Varieties Using Fluorescence and Hyperspectral Indices. *Remote Sensing*, 6, 64-86. https://doi.org/10.3390/rs6010064.

Zhang, H., Li, J., Liu, Q. H., Lin, S. R., Huete, A., Liu, L. Y. Croft, H., Clevers, J. G. P. W., Zeng, Y. L., Wang, X. H., Gu, C. P., Zhang, Z. X., Zhao, j., Dong, Y. D., Mumtaz, F., Yu, W. T. (2022). A novel red-edge spectral index for retrieving the leaf chlorophyll content. *Methods in Ecology and Evolution*, 13, 2771–2787. https://doi.org/10.1111/2041-210X.13994

Zarco-Tejada, P.J., Miller, J.R., Mohammed, G.H., Noland, T.L., & Sampson, P.H. (2002). Vegetation stress detection through chlorophyll a + b estimation and fluorescence effects on hyperspectral imagery. *Journal of Environmental Quality*, 31(5), 1433–1441. https://doi.org/10.2134/jeq2002.1433

Zhang, R., Yang, P., Liu, S., Wang, C., & Liu, J. (2022). Evaluation of the Methods for Estimating Leaf Chlorophyll Content with SPAD Chlorophyll Meters. *Remote Sensing*, 14, 5144. https://doi.org/10.3390/rs14205144